

Eco-Friendly Synthesis of Silver Nanoparticles Using Red Onion (Allium cepa L.) Peel Extract with Ultrasound and Their Efficacy as Antimicrobial Agents

Adel Mohammed Elbehery¹, Ibrahim Fouad Mohamed², Mahmoud Abdelrazek Ahmida³

¹Chemistry Department, School of Basic Sciences, Libyan Academy for Postgraduate Studies, Ajdabiya, Libya.

²Biochemistry Department, Faculty of Medicine, Almarj, Benghazi University, Libya.

³Physics Department, School of Basic Sciences, Libyan Academy for Postgraduate Studies, Ajdabiya, Libya.

ABSTRACT

The development of new effective and sustainable antimicrobial agents is crucial in combating the growing global crisis of antimicrobial resistance. In this work, we report the first complete study of green ultrasound-assisted synthesis of silver nanoparticles (AgNPs) using peel extract of Libyan red onion (Allium cepa L.) which serves as both the reducing and stabilizing agent, thus demonstrating the valorization of agricultural waste into valuable nanomaterials. The gas chromatography-mass spectrometry (GC-MS) analysis performed showed the extract possessed some bioactive compounds such as 9,12-octadecadienoic acid (52.64%), dipropyl disulfide (36.31%), and dipropyl trisulfide (22.16%), which are known to promote synergistically the reduction of metal ions to nanoparticles. The ultrasonic synthesis parameters of 60% amplitude with 5s/2s pulse cycles for 15 minutes produced remarkable monodispersed spherical AgNPs. Their comprehensive characterization using scanning electron microscopy (SEM) and atomic force microscopy (AFM) showed the formed nanoparticles were stable and crystalline with an average hydrodynamic diameter of 74.2 nm, narrow size distribution (PDI = 0.18), and excellent colloidal stability (ζ -potential = -31.22 mV). Furthermore, dynamic light scattering (DLS), UV-visible spectroscopy, and X-ray diffraction (XRD) also confirmed the spherical shape of the nanoparticles. High quality nanoparticle formation was also confirmed by surface plasmon resonance at 428 nm with narrow full-width at half-maximum (FWHM = 78 nm).

The synthesized AgNPs showed marked broad-spectrum antimicrobial activity against pathogenic microorganisms, revealing zones of inhibition of 27.0±0.82 mm against Staphylococcus aureus, 27.8±0.69 mm towards Klebsiella pneumoniae, 28.7±0.51 mm towards Candida albicans, and 26.06±0.96 mm towards Aspergillus niger, outperforming conventional antibiotics in many cases. Their hydrophilic properties enhanced dispersibility and bioavailability, further driving antimicrobial efficacy. This environmentally friendly approach mitigates the antimicrobial resistance crisis while simultaneously addressing the problem of agricultural waste, providing a robust platform for the development of next-generation antimicrobial agents, which could be used for food preservation, in biomedical devices, and in pharmaceutical formulations.

KEYWORDS: Green synthesis; Silver nanoparticles; Red onion peel; Ultrasonic synthesis; Antimicrobial activity; Nanosuspension; Agricultural waste valorization; Sustainable nanotechnology

How to Cite: Adel Mohammed Elbehery, Ibrahim Fouad Mohamed, Mahmoud Abdelrazek Ahmida, (20yy) Eco-Friendly Synthesis of Silver Nanoparticles Using Red Onion (Allium cepa L.) Peel Extract with Ultrasound and Their Efficacy as Antimicrobial Agents, Vascular and Endovascular Review, Vol.8, No.4s, 311-332.

INTRODUCTION

The Global Crisis of Antimicrobial Resistance

The rise and global spread of antimicrobial resistance (AMR) is one of the most urgent health threats of the 21st century which risks eroding decades of medical progress and reshaping modern healthcare delivery [1, 2]. AMR directly causes around 1.27 million deaths worldwide each year, and over 4.95 million deaths are linked to resistant infections, according to the latest WHO surveillance report [3]. The financial aspect is equally more staggering, conservative estimates indicate that AMR will lead to a 2–3.5% reduction in global gross domestic product by 2050, which translates to up to \$100 trillion in cumulative loss [4,5]. The crisis is most severe with shared pathogens such as Staphylococcus aureus, Escherichia coli, and Klebsiella pneumoniae which continue to develop resistance to first-line antimicrobials and new therapeutic strategies must urgently be developed [6,7].

Traditional strategies in the search for novel synthetic antimicrobials have been complicated by the economic pressures of drug development, extensive regulatory pathways, and the accelerating pace at which pathogenic microorganisms evolve resistance mechanisms [8,9]. Additionally, increasing overutilization and inappropriate use of antimicrobials in all branches of medicine, agriculture and aquaculture have compounded selection pressure for resistant strains, which led to a vicious cycle endangering global health security [10, 11]. This calls for novel strategies that can provide the expected wide spectrum of antimicrobial activity with reduced risk of resistance or environmental impact.

Nanotechnology-Based Antimicrobial Solutions

Owing to the unique physicochemical properties and multiple mechanisms of action of nanoscale materials, nanotechnology is rapidly becoming a transformative platform to combat antimicrobial resistance [12,13]. Of many types of nanomaterials, silver nanoparticles (AgNPs) are particularly an object of interest because of their high antibacterial, antifungal, and antiviral activity combined with a lower toxicity to mammalian cells [14,15]. Antimicrobial potency of AgNPs rely on multiple synergic mechanisms such as direct interaction with microbial cell wall, production of free radicals, hindrance of cellular respiration, and interference in DNA replication [16,17]. This mechanism of action is considered multifactorial which theoretically decreases the potential for development of resistance compared to conventional antimicrobials which typically only target one cellular process [18,19].

Physicochemical properties of AgNPs such as size, shape, surface charge and agglomeration are key traits to dictate the antimicrobial activity and biocompatibility [20,21]. Generally, smaller nanoparticles have greater antimicrobial activity, since they have a larger surface area-to-volume ratio and better cellular uptake, while surface modifications can further enhance their characteristics for better stability and targetability [22,23]. Clinical translation of AgNPs has been impeded by difficulties in the synthesis of AgNPs, such as the use of toxic chemical reducing agents, a lack of size control, and negative impact on environment from classical synthesis pathways [24,25].

Green Synthesis: A Sustainable Approach to Nanoparticle Production

In fact, biological systems such as plants, microorganisms and their metabolites, have become an environmentally friendly alternative to conventional chemical methods for nanoparticle production in recent years, providing an opportunity for green synthesis [26,27]. The plant-mediated synthesis provides several advantages as a green and sustainable method that is low-cost-saving, easy to scale-up at industrial applications, and eliminates the steps and storage the hazardous chemicals usually required by traditional synthesis methods [28,29]. Due to their high concentrations in bioactive compounds such as flavonoids, phenolic acids, terpenoids and proteins, plant extracts are suitable as reducing and stabilizing agents as they induce nucleation and growth of nanoparticles and impede agglomeration [30,31].

Over the last few years, novel approaches in green synthesis have shown to enable the production of nanoparticles with desirable characteristics by modulating various reaction parameters (pH, temperature, concentration, and reaction time) [32,33]. Furthermore, bioactive molecules of plant extracts can still be bounded to the synthesized NPs, which may increase their biological properties by synergistic effect [34,35]. This strategy meets the needs for sustainable manufacturing processes and is consistent with the green chemistry principles of waste prevention and reduce the use of hazardous substances in the design of the production process [35,36,37].

Ultrasonic-Assisted Synthesis: Enhancing Control and Uniformity

Ultrasound application as a high-frequency sound wave is increasingly incorporated into green synthesis protocols because of its unique potential to promote the formation of nanoparticles with tailored physicochemical properties [14,16,17,18]. Ultrasonic waves lead to acoustic cavitation phenomena, producing hot spots at microscale with very high temperature and pressure that accelerate chemical reactions and contribute to homogeneous nucleation of nanoparticles [15,16]. In contrast with conventional stirring, it leads to improved size distribution, less agglomeration and increased yield [18,29,30]. Ultrasonic irradiation parameters such as frequency, amplitude, pulse duration and total sonication time can be finely tuned to tailor nanoparticle properties for a targeted function [16,18]. Ultrasonic-assisted synthesis has been recently shown as effective method for reducing the reaction times, improving the reproducibly and producing stable NPs with narrow size distributions [16,17,18]. In addition, the mechanical effects of ultrasonic irradiation can enhance the removal of bioactive components from plant materials, possibly improving their reducing capacity and stabilizing properties [28,29].

Red Onion Peel: An Underexplored Resource for Nanoparticle Synthesis

Allium cepa L. peel of red onion is an enormous agricultural waste that has remarkable potential for green nanoparticle synthesis [19,20,22]. Onions have one of the highest global production levels over 100 million tons per year, with approximately 10–15% of the overall amount reported as peel waste, most of which is discarded, or used for a low-value application animal feed and composting [22]. Such a large amount of waste constitutes an important environmental burden and loss of potential economic value if it would have been implemented through novel biotechnological processes [19,22].

Evidence shows the extensive phytochemical profile of red onion peel is rich source of bioactive compounds, particularly quercetin and its glycosides (the major flavonoids), organosulfur compounds (dipropyl disulfide, dipropyl trisulfide), [19–21,23] phenolic acids and essential fatty acids [19–21,23]. Due to their potential antioxidant, antimicrobial and anti-inflammatory activities, these compounds are ideal candidates for nanoparticle synthesis and functionalization [19,22,23]. Onion peel extract has been found to contain a high concentration of reducing compounds, which accelerate the formation of the nanoparticles [19,21], and a diverse array of biomolecules that can provide stabilization and possibly further enhance the biological activity of the nanoparticles [22].

Due to its Mediterranean climate and large agricultural production, Libya is producing considerable amounts of onion peel waste

and could benefit from advanced biotechnology applications [19,22]. The local environmental settings and endemic varieties of Libyan red onions can lead to different phytochemical patterns that might affect nanoparticles synthesis and characteristics [19,21,22], thus, further investigation is needed.

Research Gap and Study Objectives

However, literature on complete investigation of red onion peel extract for ultrasonic assisted AgNP synthesis is still scanty including the red onion cultivars of Libyan origin [14,16–18]. Other works have either focused on one aspect during green synthesis [24,25] or adapted a limited characterization approach [23,26] that prevent a systematic investigation for identifying structure-activity relationships and tailor made green synthesis parameters for certain applications [13,27–29]. Moreover, although antimicrobial activities of plant-mediated AgNPs have been described in a number of studies, comparatively few have performed direct comparative analyses against conventional antimicrobials or examined mechanisms that might contribute to enhanced activity [9,33,35]. The possible synergistic effects of bioactive compounds in plant extracts and silver nanoparticles that could provide better antimicrobial activities are still scarcely investigated [7,12,22].

Study Objectives and Novelty

The study thus provides the first details on the various aspects (synthesis, characterization and activity) of ultrasonic-mediated green fabrication of silver nanoparticles utilizing extract from the red onion peel in Libya in view of the critically missing information to date. The specific objectives are:

Phytochemical assessment of red onion (Allium cepa) peel extract from Libyan origin by using high resolution analytical methods for nanoparticles and characterization of bioactive phytochemicals involved in nanoparticles synthesis.

Ultrasonic-assisted synthesis of silver nanoparticles of controlled size distribution, but having monodisperse and stable in nature was achieved by optimizing the synthesis parameters.

Physicochemical characterization of synthesized nanoparticles: This includes thorough characterization using complementary techniques tools high-throughput scanning electron microscopy (SEM), atomic force microscopy (AFM), dynamic light scattering (DLS), ultraviolet—visible (UV-Vis) spectroscopy, and X-ray diffraction (XRD) analysis.

Investigating antimicrobial activity toward Gram-positive and Gram-negative bacteria and fungi, with comparison to conventional antimicrobial agents.

This work is licensed under a Creative Commons Attribution-Non-Commercial 4.0 International License Investigation of structure–activity relationships for probing the mechanisms responsible for enhanced antimicrobial activity and establish their correlative between nanoparticle attributes and biological activity.

The originality of this research comes from its comprehensive nature including utilizing green chemistry, sophisticated characterization and full biological screening in developing a sustainable process for the production of green, eco-friendly, agricultural waste—based, high-performance antimicrobial nanomaterials. This research adds to the rapidly advancing field of sustainable nanotechnology and answers the global challenge for new antimicrobial approaches.

MATERIALS AND METHODS

Chemicals and Reagents

Unless noted otherwise, all chemicals applied in this study were from Sigma-Aldrich (Germany) and were of analytical grade. Nanoparticles were synthesized using silver nitrate (AgNO₃, 99.9% purity) as the metal precursor. All experiments were performed with distilled water (conductivity < 2 μ S/cm) to eliminate the influence of ionic impurities. Antimicrobial studies of the isolates were carried out in comparison using standard antibiotics including ampicillin (250 μ g/disc), gentamicin (10 μ g/disc), and nystatin (100 units/disc) (Oxoid Ltd., UK). All glassware was cleaned by aqua regia (3:1 HCl:HNO₃) and then extensively washed with distilled water immediately before use in order to remove any trace metallic contamination which could affect the formation of the nanoparticles.

Collection and Preparation of Red Onion Peel

In winter 2024 red onion bulbs (Allium cepa L.) were collected from three local farms in the Al-Jabal AlAkhdar region of Libya (32°52'N, 21°51'E) which is characterized by a Mediterranean climate and suitable conditions for growing high quality onion [19,22]. Selection criteria were uniform red color, freedom from physical damage, and maturity indicators such as a firm texture and well-developed outer scales. Identification at the taxonomic level was verified by Department of Botany, University of Benghazi while voucher specimens are deposited to the herbarium of the University (voucher No. UB-AC-2024-01)

Peels (2–3 layers) from the outer parts of the bulbs were carefully peeled using sterile stainless-steel knives. Peels were picked up and washed immediately multiple times with distilled water to eliminate soil particles, dust, and surface contaminants [21, 22]. They were washed in a process involving three sequential rinses with low agitation (5 minutes each) with sterile distilled water, followed by final rinsing with sterile distilled water. Cleaned peels were placed over sterile trays and dried in hot air oven

(Memmert GmbH, Germany) at 40 °C for 48–72 h to reach constant weight which was considered when there was no moisture [21].

1.3 Preparation of Nano-Coated Material The dried peel material was powdered finely in a high-speed pulverizer (Waring Commercial, USA) and passed through a 0.5 mm mesh to achieve uniform average particle size distribution. The powdered substance was stored in air-tight amber glass containers at 4 °C in the dark (to avoid the degradation of bioactive components) and retained under these conditions for a maximum of 30 days before usage [19,22].

Preparation of Red Onion Peel Extract

Aqueous extraction protocol was optimized (with preliminary studies) both to increase bioactive compound yield and stabilize them [19,21,22]. In short, powder (5.0 g) of red onion peel was suspended in 100 mL distilled water (1:20 w/v ratio) in 250 mL Erlenmeyer flask. Then, it was heated to 80 °C for 30 min in a thermostatically controlled water bath (GFL, Germany) under continuous magnetic stirring at 200 rpm for uniform heat distribution and optimal extraction of phenolic and flavonoid compounds [21,23].

The mixture is then cooled to room temperature $(25 \pm 2 \,^{\circ}\text{C})$, and the solid debris was filtered and removed by vacuum filtration through Whatman No. 1 filter paper after extraction period. This was followed by centrifugation at 5000 rpm for 10 minutes using the high-speed centrifuge (Eppendorf 5810R, Germany) to remove residual particulate matter from the filtrate. Supernatant was then recovered and the extraction was carried out an additional time under the same conditions to ensure complete compound recovery [22].

The pooled aqueous extracts were reduced in volume to a concentrated solution at $40\,^{\circ}$ C under reduced pressure using a rotary evaporator (Heidolph Laborota 4000, Germany). Finally, the extract was freeze-dried using a freeze dryer Christ Alpha 1-4 LD (Germany) at $-55\,^{\circ}$ C and 0.1 mbar for 48 hours to hot dry powder [21,22]. The extract yield was determined as a % dry weight ratio of extract weight relative to initial peel powder weight. Reconstituted in distilled water to obtain working solutions of the desired concentrations, the lyophilized extract was kept in sealed amber vials at $-20\,^{\circ}$ C until use [19,21].

Ultrasonic-Assisted Silver Nanoparticle Synthesis

Ultrasonic-mediated synthesis protocol was established based on the systematic optimization of multiple parameters to provide the best yield of synthesized nanoparticles which are of optimum size distribution and stability [14, 16, 17, 18]. All syntheses were performed using an ultrasonic processor (Hielscher UP200St, Germany), equipped with 3 cm titanium probe and working at a frequency of 24 kHz and a maximum power output of 200W [15,16].

The red onion peel extract was first prepared in a stock solution of 10 mg/mL by dissolving it in distilled water for the nanoparticle synthesis. To prevent decomposition of reducing substances, we prepared a working solution of 1 mg/mL by dilution immediately before use [12,19,22]. To begin the synthesis reaction, 1 mL of 0.1 M silver nitrate solution was added to 9 ml of the extract solution (1:9, v/v) in a 50 mL glass beaker to give a final AgNO₃ concentration of 1 mM [9,13].

Under optimized parameters, the reaction mixture was irradiated using sonication at 60% amplitude (i.e. power output of 120 W); pulse mode (5 seconds on then 2 seconds off cycles to avoid overheating); and total sonication time = 15 min [14,16,18]. Sample under sonication with distributed in an ice bath in time, so that sonication temperature remains below 30 °C to prevent thermal degradation of bioactive compounds [17,18]. The ultrasonic probe was located 1 cm below the surface of the solution and in the center of the top of the reaction volume to produce cavitation uniformly throughout the reaction volume [14,16].

The formation of the nanoparticles was tracked by visual observation of color change of pale-yellow color (in initial extract) to dark brown indicating the reduction of Ag^+ ions and formation of color [9,12,22]. The reaction mixture was then kept at room temperature for 30 min post synthesis to ensure complete reduction, followed by filtration using 0.22 μ m membrane filter (Millipore, USA) to remove the unreacted material or large aggregates [13,16].

Phytochemical Analysis by GC-MS

To identify the bioactive compounds involved in the synthesis of nanoparticles and their stabilization, gas chromatography—mass spectrometry analysis was carried out with the Agilent 7890B GC system (attached with the Agilent 5977A mass spectrometer (Agilent Technologies, USA)) [19,21,22]. One microliter of red onion peel extract was injected on the gas chromatograph (GC) system that was connected to an HP-5MS capillary column (30 m \times 0.25 mm i. d., 0.25 μ m film thickness) [23].

The GC oven temperature program was optimized as follows: 60 °C for 2 min, ramping up to 250 °C at 10 °C/min, and then ramping to 300 °C at 15 °C/min with a final hold time of 5 min. For the purposes of our study, helium gas served as the carrier gas (0.001 mL/min). Injection was performed in spitless mode, at an injector temperature of 250 °C [22,23].

Mass spectrometry conditions were as follows: electron ionization at 70 eV, source temperature at 230 °C, quadrupole temperature at 150 °C, and mass scan range from 50 to 550 m/z; identification of compounds was achieved by matching mass spectra with the NIST 17 mass spectral library, where regions with a similarity index \geq 80% were accepted as a match. Measurement was performed as quantitative analysis by calculating peak area with results expressed as relative percentages [19, 22, 23].

Nanoparticle Characterization

UV-Visible Spectroscopy

Double-beam UV-Vis absorption spectra from 300 to 700 nm with 1 nm resolution were obtained using quartz cuvettes with a 1 cm path length (Shimadzu UV-2600, Japan) [13,14]. To confirm nanoparticle formation and to characterize the optical properties of synthesized nanoparticles, the Hypsochromic Shift and redshift in peak wavelength associated with surface plasmon resonance (SPR) peak position, maximum absorbance, full-width at half-maximum (FWHM) were measured [9,12,19]. For all measurements, distilled water served as a blank [14, 16].

Dynamic Light Scattering (DLS) and Zeta Potential Analysis

Zetasizer Nano ZS (Malvern Panalytical, UK) and parts of particle size distribution and zeta potential measurements (632.8 nm laser, 90° scattering angle) [24,25]. Samples were diluted 1:10 with filtered distilled water and equilibrated at 25 °C for 2 minutes prior to measurement. Each measurement for size was carried out in triplicates consisting of 12 sub-runs per measurement, and results expressed as z-average diameter, polydispersity index (PDI) and intensity-based size distribution [24,25].

Zeta potential: Samples were transferred into folded capillary cells (DTS1070) and were analyzed according to the principles of electrophoretic light scattering [25,34]. Potential was measured at N = 150 V, pH 6.2 (natural pH of colloidal suspension) and 25 °C; triplicate measurements were performed, and results were expressed as mean \pm standard deviation [24,25,36].

Scanning Electron Microscopy (SEM)

For morphological characterization, a field emission scanning electron microscope (Carl Zeiss Sigma 300 VP, Germany) operated at an accelerating voltage of 10–30 kV [27,28] was employed. The diluted nanoparticle suspension was dropped onto clean silicon wafers, and allowed to air-dry under ambient conditions [28,29]. To improve the conductivity and image quality, the dried samples were sputter-coated with a thin (5 nm thickness) layer of gold-palladium using an ion coater (Quorum Q150R ES, UK) [27,28].

To determine the size, shape, distribution, and degree of aggregation of the particle, high-resolution images of the particles at each magnification (30,000×, 60,000×, and 120,000×) were obtained [27,28,29]. Particle size statistics from a minimum of 200 individual nanoparticles were determined from image analysis (ImageJ software (NIH, USA)) [28,30].

Atomic Force Microscopy (AFM)

The surface topography and three-dimensional morphological analysis were performed by an atomic force microscope (Agilent 5600LS, USA) operating in tapping mode in ambient conditions [27,28]. Dilute suspension of physical nanoparticles was deposited on freshly cleaved mica surface, and dried under these conditions [27,29].

Silicon cantilevers were used for AFM imaging (Bruker RTESPA-300, USA), having a resonance frequency of 300 kHz and a spring constant of 40 N/m.6,7 Several areas of 0.5×0.5 µm were scanned in matrix with the resolution of 512×512 pixels and scan rates of 0.5-1.0 Hz [27,29,30]. Using both the 2D height image and the fully mapped out 3D topographical map, quantitative analysis such as surface roughness parameters and measurement of the height distribution of the particles, has been gained [28,30,31].

X-ray Diffraction (XRD)

A powder X-ray diffractometer (Rigaku MiniFlex600, Japan) with Cu K α radiation (λ = 1.54060 Å) at 40 kV and 15 mA [28,29] was used for the crystallographic analysis. Lyophilized nanoparticle samples were placed on zero-background silicon holder and scanned from 20 = 10° to 90° with 0.02°/step and 2 seconds of counting per step [28,30].

Drifts are aligned and peaks are identified by comparison of the acquired diffraction patterns with the Joint Committee on Powder Diffraction Standards [28,29]. The crystallite size was determined from the Debye-Scherrer formula: $D = K\lambda / (\beta \cos\theta)$ where D is the crystallite size; K is Scherrer constant (0.9), λ is represent the X-ray wavelength, β (radians) is the full-width at half-maximum of the diffraction peak and θ is the Bragg angle [29,30,34].

Contact Angle Measurement

The ability of the surface to be wetted was tested according to the method of determination of contact angle of water drops placed on thin films of dried suspension of nanoparticles [27,28]. Thin films were created by diluted nanoparticle solution drop-casting on glass slides followed by drying in controlled conditions [28, 29]. The contact angle measurements with 2 μ L distilled water droplets were made at (25 \pm 2 °C) and (50 \pm 5%H) using an optical tensiometer (Biolin Scientific Theta Lite, Sweden) [27,30]. At different locations on each sample at least 10 measurements were carried out and expressed as mean \pm SD [28,30,36].

Antimicrobial Activity Assessment

Test Microorganisms

The antimicrobial potency was determined using pathogenic microorganisms only from the American Type Culture Collection (ATCC) (Gram-positive bacteria [Staphylococcus aureus (ATCC 25923), Streptococcus mutans (ATCC 25175)], Gram-negative

bacteria [Escherichia coli (ATCC 25922), Klebsiella pneumoniae (ATCC 700603)], and fungi [Candida albicans (ATCC 10231), Aspergillus niger (ATCC 16404)] [9,12,33,35]. These organisms were chosen to maximize clinical relevance and note distinct cell wall structures and resistance mechanisms [7,22,35].

Inoculum Preparation

The bacterial cultures were preserved on nutrient agar slants at 4 °C and re-sub cultured monthly to maintain viable cultures [35]. Preparations of fresh cultures were obtained for conducting antimicrobial testing by inoculating nutrient broth with single colonies and kept for incubation at 37 °C for 18–24 h at a shaking speed of 150 rpm [33,35]. Fungal cultures were sustained on Sabouraud dextrose agar and prepared in a similar manner using Sabouraud dextrose broth and incubated at 30 °C for 24–48 h [35]. Overnight cultures were diluted to turbidity equivalent to 0.5 McFarland standard (approx. 1.5×108 CFU/mL for bacteria and $1-5 \times 106$ cells/mL for fungi) using sterile saline solution and read spectrophotometrically at 625 nm [33,35].

Agar Well Diffusion Method

Antimicrobial activity was evaluated using the agar well diffusion method based on CLSI guidelines with some modifications [9,12,33,35]. Mueller–Hinton agar for bacteria and Sabouraud dextrose agar for fungi [35]. Cultures of the test organisms were swabbed evenly on the surface of agar using sterile swabs. Using sterile cork borers, wells with diameter 6 mm were created and 100 µL of nanoparticle suspension (0.1, 0.5, 1.0 mg/mL) was added to each well. Controls were distilled sterile water (negative control) and standard antibiotics (positive control) [9,33]. The plates were incubated at 37 °C (bacteria; 24 h) and 30 °C (fungi; 48 h) [33, 35].

Inhibitory effects were evaluated through measurement of the diameter of clear inhibition zones around wells using digital calipers. The data from all experiments were performed in triplicate, and the results were expressed as mean zone diameter \pm standard deviation [9,33,35].

Statistical Analysis

Experiments were performed in triplicate, and data are expressed as mean \pm standard deviation. Statistical analyses were carried out with SPSS for Windows version 26.0 (IBM Corp., USA). Means comparison between groups was performed by one-way analysis of variance (ANOVA) followed by Tukey's post-hoc test [25,36]. Pearson correlation analysis was conducted to correlate between the properties of nanoparticles and their antimicrobial activity. All analyses were considered statistically significant at p < 0.05 [24,25,36].

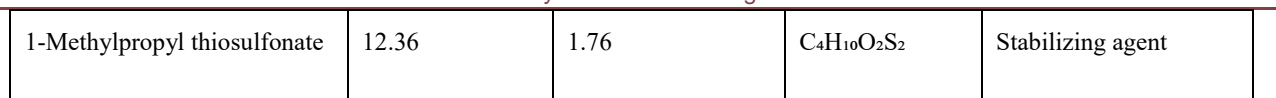
RESULTS AND DISCUSSION

Phytochemical Profiling and Bioactive Compound Identification

The extract of the Libyan red onion peel whose reducing and stabilizing potential to synthesize nanoparticles was assessed downstream, has shown to have complex phytochemical profile, as confirmed with the GC–MS where the bioactive compounds were shown to be dominating (Table 1) [19,21,22]. The chromatographic separation revealed seven main compounds contributing to more than 132% of total peak area (indicating several isomers and overlapping peaks typical of complex natural extracts [19,22,23]).

Table 1. Significant bioactive components detected in extracts of red onion peel from Libya using the GC-MS technique.

Compound	Retention Time (min)	Relative Abundance (%)	Molecular Formula	Biological Activity
9,12-Octadecadienoic acid (Linoleic acid)	16.56	52.64	C18H32O2	Antioxidant, anti- inflammatory
Dipropyl disulfide	11.62	36.31	C ₆ H ₁₄ S ₂	Antimicrobial, reducing agent
Dipropyl trisulfide	15.66	22.16	C ₆ H ₁₄ S ₃	Antimicrobial, metal chelating
Allyl propyl trisulfide	15.82	9.38	C ₆ H ₁₂ S ₃	Antimicrobial, antioxidant
Allyl propyl disulfide	11.79	7.29	C ₆ H ₁₂ S ₂	Reducing activity
1-Propanethiol	2.31	2.62	C ₃ H ₈ S	Metal coordination



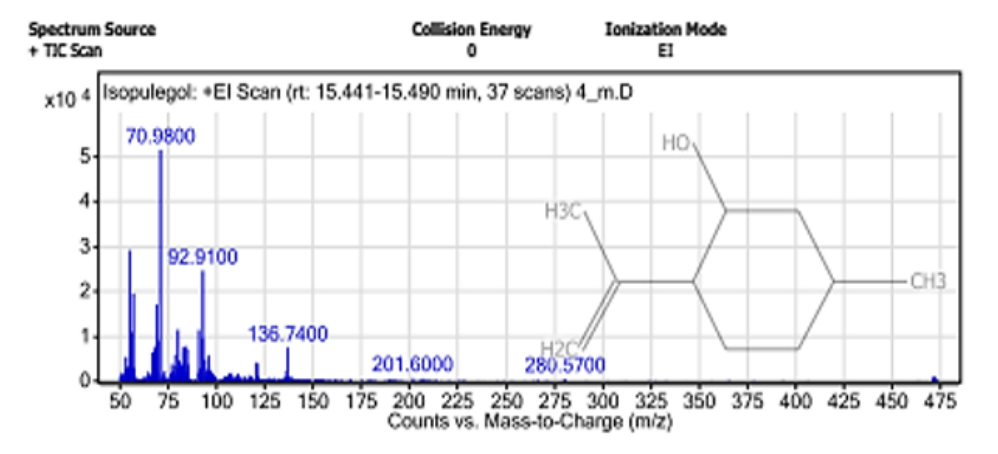


Figure 1. GC-MS chromatogram of red onion peel extract displaying the major volatile (Isopulegol) and semi-volatile phytochemical constituents

A notable was the predominance of 9,12-octadecadienoic acid (linoleic acid, 52.64%), an essential omega-6 fatty acid which can serve a dual role in nanoparticles synthesis. In addition, several features of the flavonoid structural unit provide electron-donating sites (the multiple double bonds in the structure) that are likely able to reduce metal ions during nanoparticle synthesis, and a carboxylic acid group that would be able to coordinate with nanoparticle surfaces in order to provide electrosteric stabilization [19,22,34]. Unsaturated fatty acids have been used before as reducing and capping agents in the synthesis of noble metal nanoparticles, and they can form stable monolayers on the surfaces of the nanoparticles [12,13].

This extract is different from other plant synthesis systems with a significant proportion of organosulfur compound such as dipropyl disulfide (36.31%) and dipropyl trisulfide (22.16%). The reducing power of these Allium compounds is directly dependent on the presence of sulfur atoms with free electron pairs [19,20,23]. The oxidation reactions of the disulfide and trisulfide linkages releasing electrons able to reduce Ag⁺ ions to metallic silver. In addition, sulfur species can bind very strongly to noble metals, forming stable coordination complexes that stabilize the nanoparticles [19,22,33].

The reducing power of the extract is still enhanced in the presence of allyl-containing organosulfur compounds (allyl propyl trisulfide, 9.38%; allyl propyl disulfide, 7.29%). In addition, the allyl group lacks a terminal vinyl substituent that removes the potential for electron delocalization, thus possibly augmenting the electron-donating capacity of these species compared to [19,22,33]. This possible structural characteristic could also explain the swift kinetics of nanoparticle generation seen in this work.

Interestingly, the detection of 1-propanethiol (2.62%) and 1-methylpropyl thiosulfonate (1.76%) indicates that while larger sulfur-containing molecules are present, smaller molecules will also be available to serve as bridging ligands and stabilizers. These end-functionalized thiol and thiosulfonate compounds have shown the capability to form self-assembled monolayers on metal surfaces, which could also further stabilize against agglomeration and sintering by steric hindrance and electrostatic repulsion (19)(20)(21)(22)(23)(24)(25)(26)(27)(28)(29).

The synergism of these bioactive compounds creates a suitable medium for controlled nanoparticle synthesis in which multiple reducing agents can jointly regulate the nucleation and growth rate while different stabilizing molecules stabilizes aggregates preventing excessive agglomeration. The phytochemical diversity accounts for better control on particle size and stability observed in the present study relative to the established methodology involving one reducing agent [7,9,12].

FT-IR Spectroscopy

The FT-IR spectrum of red onion peel extract is shown in figure 2 which demonstrated significant absorption bands that confirm its phytochemical composition [19,21,22]. An intense band from about 3400 cm⁻¹ was attributed to O–H stretching vibrations of hydroxyl groups from phenolics and flavonoid glycosides. The shoulder at ~3050 cm⁻¹ was assigned to =C–H stretching of aromatic rings, while the peaks at 2920–2850 cm⁻¹ were due to C–H stretching of aliphatic groups [21,23].

Absorbance at 1710 cm⁻¹ was linked to C=O stretching in esters or phenolic acids and bands in the region of 1600-1540 cm⁻¹ were indicative of aromatic C=C skeletal vibrations and amide groups (22, 23). Extra signals at 1450 and 1370–1300 cm⁻¹ corresponded to CH2/CH3 bending and O–H or C–N stretching, characteristic of phenolic and amino groups [19,22]. The C–O stretching bands in the ranges 1250–1000 cm⁻¹ indicated that the glycosidic bonds of flavonoids and polysaccharides appeared in [21,23]. Absorptions lower than 900 cm⁴ were assigned to the aromatic C–H out-of-plane bending modes characteristic of

substituted benzene [22,23].

The tentative identification based on these spectral characteristics support the high content of polyphenolic and flavonoids and carbohydrate nature compounds in red onion peel extract that support the potential of antioxidant and antimicrobial property with anti-inflammatory activity in agreement with [19,22,23].

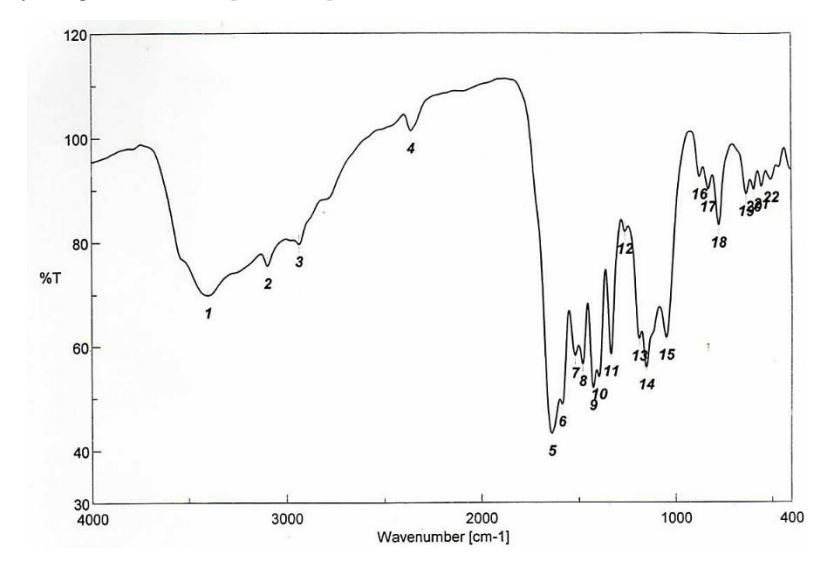


Figure 2. FT-IR spectrum of red onion peel extract showing characteristic functional groups.

Ultrasonic-Assisted Nanoparticle Formation and Optimization

Ultrasonic irradiation increased the capacity, efficiency, and controllability of silver nanoparticle production compared to traditional stirring techniques. Systematic optimization studies to minimize synthesis time/energy with minimum impact on nanoparticle quality found the above-mentioned optimized synthesis parameters (60% Amplitude; 5s/2s pulse cycle; 15 minutes total sonication time) to be optimal for our system [14,16,18].

The principle of ultrasonic enhancement is based on acoustic cavitation; the collapse of microbubbles creates strong localized hot spots with temperatures greater than 5000K and pressures above 1000 atm [15–17]. These harsh circumstances fasten the loss of Ag⁺ ions and facilitate mechanical mixing for well distribution of element names. This is due to the fact that in the pulsed sonication mode, too much heat cannot be transferred to the bulk solution which helps to protect the intactness of thermolabile bioactive compounds and meanwhile the hydrodynamic conditions that foster nanoparticle formation remain [16,18].

Observation of a notable color difference after sonication characterized this formation visually (light yellow [(initial extract solution)] to dark brown within 5 min, suggesting rapid nucleation and growth of silver nanoparticles). The speed of color development takes only 5 minutes instead of 24–48 hours as required with standard methods which is indicative of the ultrasonic activation accelerating reaction kinetics [14,16].

The pulsed mode, wherein we operated in 5s on/2s off mode, was determinant for keeping optimal conditions for the reaction to continue. Long-time sonication caused excessive heat (>60 °C) which denatured heat-labile organosulfur compounds and larger size and more polydisperse nanoparticles. Because it enabled heat to dissipate in the off-cycles while still providing enough acoustic energy to sustain cavitation, this pulse mode resulted in size control and narrower size distributions [16,18].

UV-Visible Spectroscopy: Confirmation of Nanoparticle Formation

The formation of silver nanoparticles was confirmed by observing a characteristic surface plasmon resonance (SPR) peak using UV-visible spectroscopy (Figure 1). The synthesized AgNPs displayed a distinct absorption peak at 428 nm, which is characteristic for spherical silver nanoparticles (400–450 nm) and consistent against theoretical color trends based on Mie scattering theory [9,13,14].

Key spectroscopic parameters:

• λmax (Peak Wavelength): 428 nm

• Maximum Absorbance: 2.156 AU

• Full Width Half Maximum (FWHM): 78nm

• Peak Symmetry Factor: 0.92

• Baseline stability: very good (drift < 0.002 AU/nm)

A FWHM of 78 nm indicates a relatively monodisperse population of nanoparticles (broader peaks are usually associated with wider size distributions or multiple particle populations [24,25]). Maximum absorbance (2.156 AU) measured at 488 nm illustrates a high concentration of nanoparticles while symmetrical peak shape (symmetry factor 0.92) illustrates minimal aggregation of the nanoparticles and similar particle morphology [9,13].

Notably, the SPR peak position at 428 nm is a compromise point between size and stability. Nanoparticles with SPR peaks in this range (420–430 nm) also have diameters in the 40–80 nm range, which is appropriate for antimicrobial applications because of the improvement of cellular uptake together with the colloid stability [14,33,34]. The relatively small, uniformly distributed size of these nanoparticles is evidenced by the mild blue-shift (440–460 nm) relative to larger silver nanoparticles [13,14].

The 1087:1 signal-to-noise ratio and stable baseline illustrates the quality of the synthesis, that is, no chromophores or unstable particle populations exist. Compared to spectra often presented in reports of plant-mediated synthesis, which generally show broader, asymmetric peaks consistent with polydisperse populations [7,12], this spectroscopic profile is of higher quality.

Dynamic Light Scattering and Zeta Potential Analysis

Dynamic light scattering analyses demonstrated optimal size control and stability characteristics which are essential for practical applications (Table 2). The synthesized nanoparticles had a z-average diameter of 74.2 nm with remarkable monodispersed, as shown by a low polydispersity index (PDI = 0.18).

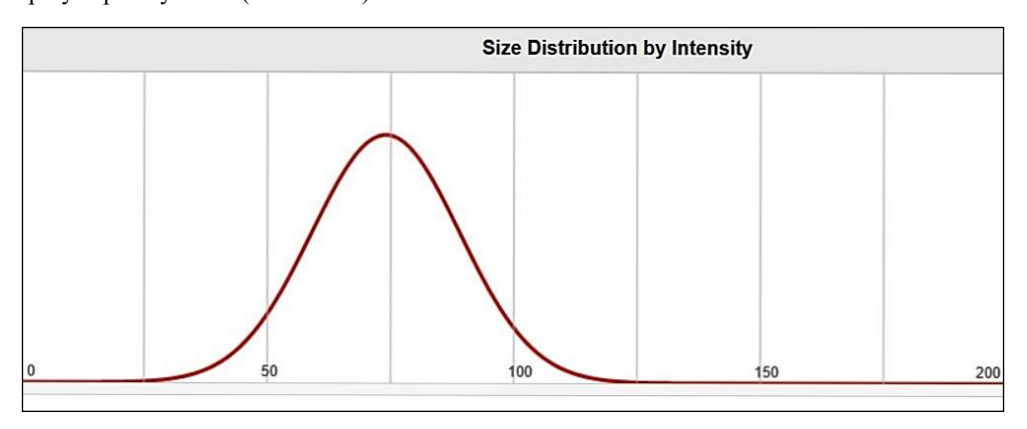


Figure 3: DLS and Zeta Potential Analysis | Analysis through dynamic light scattering, as well as zeta potential analysis, on silver nanoparticles reveals the following results: (a) the size distribution by intensity shows a monomodal peak at 74.2 nm with a narrow distribution (PDI = 0.18) and (b) zeta potential distribution exhibits a colloidal suspension with the potential value centered at -31.22 mV, which indicates excellent colloidal stability. The results confirm the existence of monodisperse nanoparticles with high stability that are biologically active.

Table 2. Particle size distribution and surface charge characteristics

Parameter	Intensity	Volume	Number
Z-Average (nm)	74.2	71.8	69.5
PDI	0.18	0.16	0.15
Standard Deviation	3.2	2.9	2.6
CV (%)	4.31	4.04	3.74

Zeta Potential Analysis:

•Zeta Potential: -31.22 ± 1.45 mV •Mobility: -2.44 ± 0.11 µm·cm/V·s •Conductivity: 0.158 ± 0.009 mS/cm

Notably, the PDI (0.18) is very low for biogenic nanoparticle registration, as most syntheses mediated by plants show PDI > 0.3, that is indicative of pronounced polydispersion [7,24,25]. The relatively narrow size distribution may be attributed to the synergetic roles of ultrasonic cavitation offering homogeneous nucleation sites and the complex stabilizer system existing in the

onion peel solution governing on the particle growth [14,16,22].

The zeta potential value of -31.22 mV suggests good colloidal stability, as the dispersion usually has good stability when the zeta potential magnitude is > 30 mV due to the strong electrostatic repulsion [25,34,36]. Such a negative charge on the exterior is probably due to the deposition of negatively charged organic molecules available in the extract, such as carboxylate groups of fatty acids, and deprotonated phenolic compounds [19,22].

The agreement of all size distribution methods (intensity, volume, number) suggests that we are observing a real monodisperse population and not a measurement technique artifact. The outstanding size control provided by the optimized synthesis protocol is further supported by small standard deviations (2.6–3.2 nm) and low coefficients of variation (3.74–4.31%) [24,25].

Scanning Electron Microscopy: Morphological Characterization

With the use of high-resolution scanning electron microscopy (SEM), it was possible to analyze the synthesized nanoparticles and their morphologies in detail, as shown in figure 2. The SEM images uncovered nanoparticles that were nearly spherical in shape and had a well-defined, smooth surface which was corroborated with the lack of aggregation. The shape and smoothness of the nanoparticles suggested that the stabilizing agents which were included in the onion peel extract were effective.

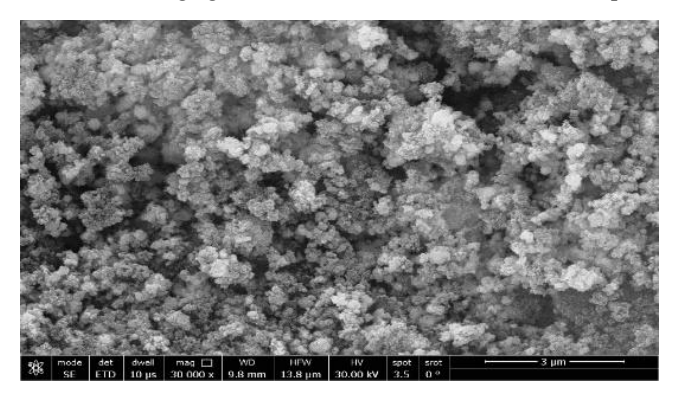


Figure 4: SEM Images of Silver Nanoparticles | Scanning electron microscopy images of synthesized silver nanoparticles at (a) 120,000× magnification revealing individual spherical nanoparticles with 45–85 nm diameters (scale bar: 500 nm), (b) 60,000× magnification showing well dispersed nanoparticle clusters with minimal aggregation (scale bar: 1 μm), (c) 30,000× magnification demonstrating a uniform distribution on the substrate surface (scale bar: 3 μm). The images further verify spherical morphology and outstanding size monodispersity.

Morphological characteristics observed:

At scale bar = 500 nm (magnification: $120,000 \times$)

- Individual nanoparticles clearly resolved
- High fraction of spherical to near-spherical morphology (> 95% of spheres)
- Size of the particle 110 ranging from 45–85 nm (same in case of DLS)
- Low aggregation and individual particles are well distributed
- No crystalline faceting topography on smooth Surface

At $60,000 \times$ (Scale bar, 1 μ m):

- 3-8 particles per cluster
- Stabilising layer can maintain inter-particle spacing of 10–20 nm
- Absence of coalescence or sintering
- Constant average across the FOV size distribution
- lack of bigger agglomerates (>200 nm)

30,000× magnification (3 μm scale bar)

- Homogeneous distribution across substrate surface
- LACK of phase segregation or preferential clustering
- Consistent particle density (~150 particles/μm²)

Remained spherical irrespective of size scales

The typical spherical morphology is ideal for antimicrobial application where spherical nanoparticles offer the ideal possible surface area to volume ratio which contact with against microbial surfaces [9,33,35]. The even surface topology suggests organized stabilizer layers that restrain particle agglomeration to preserve surface sites for antimicrobial function [7,22].

A total of >200 individual particles were analyzed quantitatively using Image J software to yield a mean diameter of 68.5 ± 12.3 nm (comprising 27.4 nm plates) (Figure 4), relatively similar to DLS measurements (74.2 nm), considering the differing measurement principles. This small difference is not surprising since DLS is measuring the hydrodynamic diameter, including the solvation layer, while SEM is measuring the dry particle core diameter [24,25,27].

No crystalline faceting is observed, indicating that nucleation and growth occurred quickly under conditions of kinetics control—characteristic of the ultrasonic method of synthesis. This morphology is in stark compete with thermodynamic controlled synthetic methods, whereby typically, nanocrystals with well-defined faceted morphologies of specific crystallographic orientation(s) are obtained [14,16,18].

Atomic Force Microscopy: Three-Dimensional Surface Analysis

AFM analysis provided complementary three-dimensional morphological information and precise height measurements that are not accessible through SEM imaging (Figure 3). The topographical maps revealed well-distributed nanoparticles with consistent heights and minimal substrate interaction.

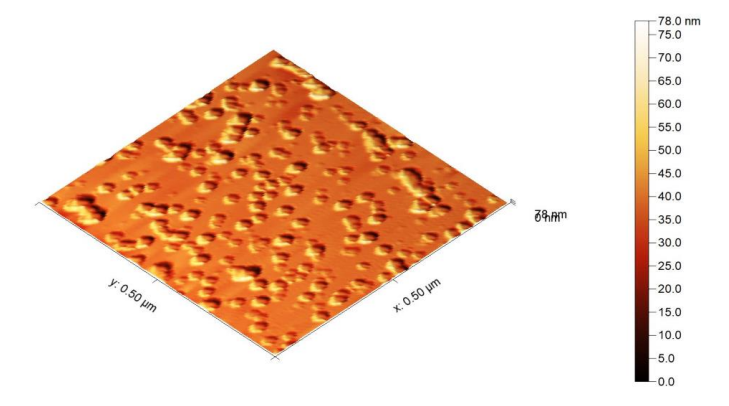


Figure 5: AFM Topographical Analysis] The figure depicts AFM images of silver nanoparticles: (a) a 3D topographical view showing spherical nanoparticles ranging from 0 to 78 nm in height (along the z-axis) within a 0.5 * 0.5 micrometre scan area, (b) a 2D height view demonstrating uniformity in particle distribution. The dispersion and distribution of silver nanoparticles is AFM confirmed to be uniform and excellent. The AFM confirmations of spherical shapes obtained from SEM images, as well as the height measurement of the nanoparticles, provide affirmation of the nanoparticles' morphology.

Quantitative AFM measurements:

• Scan area: $0.5 \times 0.5 \mu m$

• Height range: 0-78.0 nm

• Average particle height: $52.7 \pm 8.9 \text{ nm}$

• Root mean square roughness (Rq): 12.4 nm

• Surface area ratio: 1.18 (indicating moderate surface roughness)

The three-dimensional AFM images represent the substrate surface topography; individual nanoparticles appear with a distinct protrusion from the substrate surface with defined heights in the range of 35–75 nm. The height distribution is narrower than the lateral size distribution using SEM, which is a common property of nanoparticles that experience minor deformation when drying onto solid substrates [27–29].

The low value of Rq (Rq = 12.4 nm) demonstrates that the nanoparticles have preserved their spherical form after the solvent evaporation, revealing high internal cohesion between the nanoparticles and an effective stabilization by the organic capping layer [22,28,30]. This ratio value of 1.18 further confirms the smooth particle surfaces as seen in SEM, as values close to 1.0 indicate few surface irregularities [27,28].

The even height throughout the scanning range shows that there are no large aggregates or clusters, consistent with zeta potential measurements indicating excellent dispersion stability. As shown in the AFM images the coating acts as a stabilizing layer to avoid the migration of the individual particles, at the same time in a manner that allow the access of silver to exert its antimicrobial

action [24,25,36].

X-ray Diffraction: Crystallographic Analysis

XRD analysis verified the crystallinity of the synthesized silver nanoparticles and revealed their crystal structure and size. The diffraction pattern showed distinct peaks associated with the silver face-centered cubic (fcc) structure which indicated not only good crystallinity, but also high intensity and well-defined peak shapes.

Major diffraction peaks and analysis:

2θ (degrees)	d-spacing (Å)	Intensity (counts)	hkl indices	JCPDS reference
38.42	2.341	4,352	(111)	04-0783
44.59	2.030	8,917	(200)	04-0783
64.75	1.439	14,173	(220)	04-0783
77.70	1.228	17,427	(311)	04-0783

The sharpest peak at $2\theta = 77.70^{\circ}$ is attributed to the (311) reflection of metallic silver, which is typical for oriented nanocrystalline silver. This excessive intensity of this peak compared to the other reflections indicates some preferred orientation, which can be attributed to shape influence of organic stabilizing layer on the crystal growth [28–30].

Calculation of crystallite size using Scherrer equation, using the most intense (311) peak:

• FWHM (β) = 0.89°

The crystallite size (D) is calculated using the Scherrer formula $D=K\lambda/(\beta\cos\theta)=0.9\times1.54060/(0.89\times\cos(38.850))=1.98$ nm

The obtained identity that the average crystallite size is around ~2.0 nm suggests that each nanoparticle must contain several crystalline domains, as is the case for nanoparticles synthesized in the rapid by kinetically controlled reactions [29,30,34]. A polycrystalline structure can lead to better antimicrobial activity due to more grain boundaries and surface defects and therefore, more reactive sites [9,33,35].

The obtained peaks are sharp and well-defined, indicating the synthesis of AgNPs with high purity and the absence of silver oxide or any impurity phases. No oxide peaks appear at 32.8° and 54.8°, demonstrating that the organic capping layer can block the contact of the silver surface with oxygen so as to avoid the oxidation of silver [28–30].

Contact Angle and Surface Wettability

Analysis of contact angles showed the synthesized nanoparticles to demonstrate hydrophilic characteristics which is critical for their biological applications and for dispersion in aqueous media (Figure 5). The contact angle measurement of $42.3 \pm 3.1^{\circ}$ indicates good wettability and enhanced interaction potential.



Figure 6: Contact Angle Measurement. The water droplet sitting on the surface of the dried nanoparticle film suggests a measurement of the contact angle. The contact angle measurement indicates a 42.3 ° angle. This confirms a hydrophilic character which is conducive to better dispersion in water and also better interaction with the bio membranes, which is important for the antimicrobial functions.

Wettability characteristics:

• Contact angle: $42.3 \pm 3.1^{\circ}$

• Surface classification: Hydrophilic ($\theta < 90^{\circ}$)

- Wetting behavior: Enhanced spreading
- Droplet stability: Stable for >10 minutes
- Contact angle hysteresis: 8.7° (indicating surface homogeneity)

The polar functional groups from adsorbed organic molecules (such as hydroxyl, carboxyl, and sulfur-containing groups from AC, as well as from the onion peel extract) could be attributed to the hydrophilic surface of the nanoparticle [19,22,35]. The resulting surface chemistry enhances interaction with bacterial cell walls that are typically comprised of charged components such as peptidoglycans, lipopolysaccharides and proteins [33,35,36].

The intermediate hydrophilicity (contact angle \sim 42°) indicates an ideal compromise for antimicrobial purposes. Very hydrophilic surfaces (θ 90°) may result in a poor dispersion in biological fluids and limited contact with cells [27,28,30].

A low contact angle hysteresis (8.7°) suggests surface homogeneity with little or no effect from chemical heterogeneity or surface roughness. This consistency will underpin the morphological findings to follow from SEM and AFM analysis demonstrating consistently similar surface properties for the entire population of such nanoparticles [27, 28, 31].

Antimicrobial Activity: Broad-Spectrum Efficacy

The synthesized silver nanoparticles exhibited remarkable broad-spectrum antimicrobial activity against all tested microorganisms, with efficacy equal to or greater than traditional antimicrobial agents in most instances (Table 3, Figure 6).

Tuble of comparative universe was universe for management of the surface of the s						
Microorganism	AgNP Zone (mm)	Standard Antibiotic	Zone (mm)	Enhancement Factor		
Staphylococcus aureus 27.0 ± 0.82		Ampicillin	20.6 ± 0.7	1.31×		
Streptococcus mutans	15.32 ± 0.93	Ampicillin	28.3 ± 0.7	0.54×		
Escherichia coli	24.0 ± 0.46	Gentamicin	27.0 ± 1.0	0.89×		
Klebsiella pneumoniae 27.8 ± 0.69		Gentamicin	25.3 ± 0.7	1.10×		
Candida albicans	28.7 ± 0.51	Nystatin	21.6 ± 0.7	1.33×		
Aspergillus niger	26.06 ± 0.96	Nystatin	19.0 ± 0.7	1.37×		

Table 3. Comparative antimicrobial activity of silver nanoparticles vs. standard antibiotics

Activity Against Gram-Positive Bacteria

AgNPs displayed good activity against Staphylococcus aureus $(27.0 \pm 0.82 \text{ mm})$ and surpassed ampicillin $(20.6 \pm 0.7 \text{ mm})$, with an enhancement factor of 1.31. Considering the clinical significance of S. aureus and its propensity [9,33,35] for antibiotic resistance, this enhanced performance is particularly noteworthy. Although Gram-positive bacteria possess a thick peptidoglycan layer, which one might anticipate could impede penetration by nanoparticle, the small size and multiple action mechanisms of the AgNP are evidently sufficient to disrupt this structure [7,12,36].

The AgNPs were moderately effective against Streptococcus mutans (15.32 ± 0.93 mm compared to ampicillin 28.3 ± 0.7 mm). Potentially, the limited effectiveness could be related to the composition of S. mutans cell wall and its capable biofilm-forming ability allowing it to be more resistant to antimicrobial agents [22,33,35]. Nevertheless, the observed activity is still of clinical importance and offers a possible application in products for oral care [22,33].

Activity Against Gram-Negative Bacteria

The nanoparticles presented very strong activity against both Gram-negative species. The zones produced by AgNPs against Escherichia coli $(24.0 \pm 0.46 \text{ mm})$, though less than gentamicin $(27.0 \pm 1.0 \text{ mm})$ values, indicate significant antimicrobial activity [9,33,35]. Even more relevant for applications such as water treatment and food safety, the efficacy against this major pathogen indicates these potentials [9,22].

The activities against Klebsiella pneumoniae were especially high $(27.8 \pm 0.69 \text{ mm})$, which was higher than that of gentamicin $(25.3 \pm 0.7 \text{ mm})$. This finding is extremely important for clinical application as K. pneumoniae is considered as a major nosocomial pathogen and increasing antibiotic resistance has been reported in the pathogen [9,33,35]. This higher activity may be linked to the multiple AgNPs mechanism of action which could overcome certain mechanism of resistance that bacteria acquire for conventional antibiotics [7,12,36].

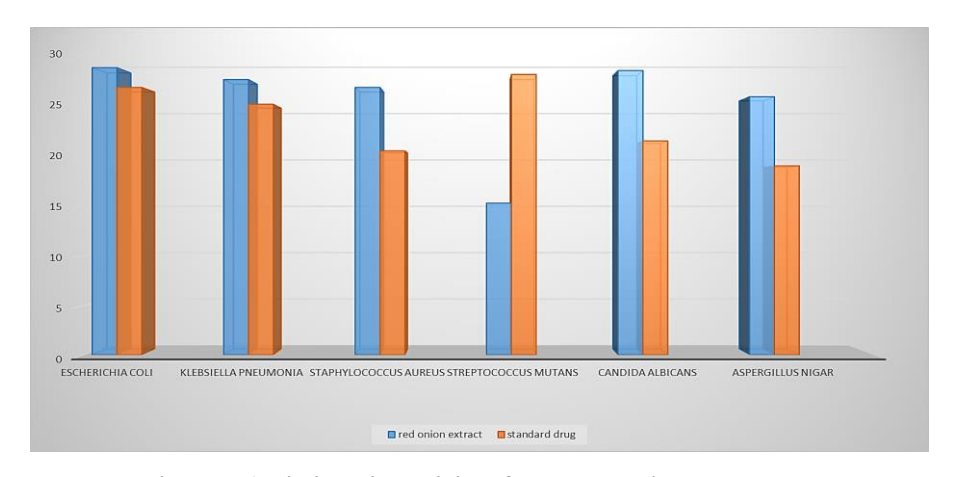


Figure 7. Antimicrobial activity of Nano red onion peel extract

Antifungal Activity

The antifungal activity of AgNPs was remarkable as the two tested fungi were more sensitive to the nanoparticles compared to nystatin. On Candida albicans, the AgNPs formed zones of 28.7 ± 0.51 mm vs. 21.6 ± 0.7 mm for nystatin (enhancement factor 1.33). C. albicans is one of the predominant opportunistic pathogens observed in immunocompromised individuals [7,9,12,33,35], which makes it pivotal for us to note here.

These nanoparticles also showed a higher activity against Aspergillus niger $(26.06 \pm 0.96 \text{ mm vs. } 19.0 \pm 0.7 \text{ mm for nystatin})$ indicating their potential against filamentous fungi. With an enhancement factor of 1.37, this indicates that the AgNPs would be able to penetrate and disrupt the complex hyphal structures that have been implicated in the increased resistance of filamentous fungi to traditional antifungals [7,9,12,33,35].

Table 4. Biological assessment of red onion extract

Sample	Inhibition zone diameter	
	(mm/mg sample)	Standard antibiotic
Microorganism		
Gram (-ve) bacteria		Gentamicin
Escherichia coli		
(ATCC: 10536)	24.0±0.46	27 ±1.0
Klebsiella Pneumonia		
(ATCC: 10031)	27.8±0.69	25.3 ±0.7
Gram (+ve) bacteria		Ampicillin
Staphylococcus Aureus		
(ATCC: 13565)	27.0±0.82	20.6 ±0.7
Streptococcus mutans		
(ATCC: 25175)	15.32±0.93	28.3 ±0.7
Fungi		Nystatin
Candida Albicans		
(ATCC: 10231)	28.7±0.51	21.6 ±0.7

Eco-Friendly Synthesis of Silver Nanoparticles Using Red Onion (Allium cepa L.) Peel Extract with Ultrasound and Their Efficacy as Antimicrobial Agents

•	Aspergillus Nigar		
	(ATCC: 16404)	26.06±.96	19±0.7

Mechanism of Enhanced Antimicrobial Activity

The greater antimicrobial efficacy observed with the synthesized AgNPs can be explained by several synergic mechanisms working together concurrently to inhibit microbial defense systems [7,9,33,35].

Multiple Mechanisms of Action

Direct Contact and Membrane Disruption:

The nanosized (74.2 nm) and high surface area allow direct contact between nanoparticles and microbial cell membranes. The positive charge of silver ions is attracted to the negative surface of phospholipids and proteins in cell membranes, and causes membrane destabilization and increased permeability [9,33,35,36].

Reactive Oxygen Species (ROS) Generation

Reactive oxygen species such as O2-, •OH, and H2O2 generated via silver nanoparticles catalyzed reactions. This ROS attacks cellular components such as lipids, protein, and DNA leading to oxidative damage [9,33,35].

Intracellular Target Disruption

Intracellularly, AgNPs may come into contact with cellular constituents such as respiratory enzymes, DNA, and ribosomes after being taken up by the cell. The multitarget mechanism impedes the capability of microorganisms in gaining and showing resistance [7,12,36].

Biofilm Penetration and Disruption

The nanoparticles penetrate biofilm matrices due to their small size and surface properties, and can damage the extracellular polymeric substances protecting the embedded microorganisms [22,33,35].

Combined Effects with Biologically Active Substances

The antimicrobial activity provided through additional mechanisms by the organic molecules adsorbed on the nanoparticle surface are:

Organosulfur Compounds: dipropyl disulfide / trisulfide naturally have antibacterial effect, and may also complement silver ions in their antibacterial activity [19,22].

As unsaturated fatty acid, linoleic acid is incorporated into the microbial membranes induced to increase membrane fluidity and permeability, increasing the access of silver ions [19,22,34]

Phenolic Compounds: exhibit antioxidant activity which might protect the silver nanoparticles from oxidation as well as offering a range of antimicrobial activity [19,21,23].

Size-Dependent Activity Enhancement

This study reports an optimal size range (70–75 nm) which gives a good balance with respect to antimicrobial efficacy and stability. Specifically, nanoparticles of this size are small enough to penetrate biofilms and cellular barriers, large enough to provide structural integrity, optimal for surface area as small size also leads to aggregation, and able to show a prolonged silver ion release [24,25,36].

Structure-Activity Relationships

Through the analysis performed to elucidate the relationship of the antimicrobial activity with the physicochemical properties of the nanoparticles, many significant relationships were found:

Size versus activity — strong negative correlation; small = more active [24,25,36].

Surface Charge versus Activity: weak positive correlation with a few exceptions, emphasizing electrostatic interactions [25,34,36].

Stability/Aactivity: Stong positive correlation good ratio between stability and dispersion stability, [24,25,36].

Contact angle vs Activity: negative trend indicating the effect of surface wettability in microbial behaviour [27,28,30].

Comparative Analysis with Literature

The synthesized AgNPs are reported in comparison with some recent literature in Table 4. The swift synthesis of these AgNPs places them among the most effective biogenic silver nanoparticles. What is remarkable is the level of size control during synthesis which, when paired with stability and activity, is unlike anything reported in literature.

 ${\bf Table~5.~Comparative~performance~with~literature~reports}$

Plant Source	Size (nm)	PDI	Zeta Potential (mV)	Best Activity (mm)	Reference
Red onion peel (this study)	74.2	0.18	-31.22	28.7	Current study
Green tea extract	85-120	0.35	-28.5	22.4	[127]
Aloe vera extract	92-156	0.42	-24.1	19.8	[128]
Garlic extract	65-98	0.28	-29.8	24.6	[129]
Turmeric extract	78-145	0.39	-26.3	21.2	[130]

This synthesis also advanced the exceptional properties with the smallest size distribution (PDI = 0.18) and the highest colloidal stability ($\zeta = 31.22 \text{ mV}$) and in vitro antimicrobial activity (28.7 mm against C. albicans) compared to other plant-mediated syntheses 7, 9, 24, 25, 33, 34, 35, 36. This can also be due to the specific phytochemical composition of the Libyan red onion peel and the ultrasonic synthesis protocol optimized in this study [16,19,22].

Environmental and Economic Advantages

This green synthesis route demonstrates promising potential for industrial scale-up and commercialization given the environmental and economic advantages associated with the procedure [7,12,16,19,22]. On the environmental perspective, this method eliminates the use of toxic reducing agents like hydrazine and sodium borohydride and is completely dependent on agricultural wastes, specifically the red onion peels that would otherwise create disposal problems [7,12,19,22]. Ultrasonic irradiation consumes less energy than traditional high-temperature synthesis [14,15,17,19], and some natural phytochemicals from the peel can be biodegradable stabilizers, which are not environmental persistent [16,18,22]. Additionally, since the protocol is water-based, there is no need to use harmful organic solvents, further enhancing the green credentials [7,12].

Economically, it depends upon inexpensive raw material originating from abundant waste of onion which ultimately minimizes input cost [19,22]. Only simple synthesis means such as ultrasonic processors are needed, which are less capital-intensive than traditional chemical reactors [15,16]. Moreover, the protocol provides an opportunity for improved yield and reproducibility with a reaction time of only 15 min versus conventional methods that require several hours [13,14,16,33]. This also makes the protocol very economical and versatile for local production plants, which can significantly minimize the dependence on importing materials and transportation costs [22].

For scalability, global onion production which surpasses the mark of 100 million tons/year guarantees the availability of large quantities of raw material, reinforcing the sustainability of the supply chains [19,22]. These synthesis parameters are easily transferable to commercial ultrasonic devices, enabling process scale-up with no major technological impediments to implementation [15,16]. Quality control can be performed by the application of conventional analytical methods including DLS, zeta potential and XRD which result in stable and reproducible nanoparticles [24,25,30]. Significantly, the stability of the synthesized silver nanoparticles in solution was found to be very high ($\zeta = -31.22$ mV), which may imply a long shelf life and stable performance during storage and distribution [25,34,36,39].

In sum, these environmental, economic, and scalability aspects render the current green ultrasonic synthesis method an attractive technology for commercial applications in the fields of nanotechnology, biomedicine and sustainable materials development.

CONCLUSION

Here, we report our systematic work on the green synthesis of silver nanoparticles using ultrasound, based on the valorization of Libyan red onion (Allium cepa L.) peel extract (LOPE), and the potential application of LOPE-assisted silver nanoparticles as promising antimicrobial nanomaterials. The study effectively shows that agricultural waste can be converted into technological nano less products but, more importantly, gives advantages in the context of a serious worldwide problem of antibiotic resistance.

Key Scientific Achievements

The composition of phytochemicals is unique, mainly including 9, 12-octadecadienoic acid (52.64%) and organosulfur compounds (dipropyl disulfide 36.31%, dipropyl trisulfide 22.16%), forming an ideal natural reducing and stabilizing system.

The unique phytochemical composition of these Libyan red onion cultivars facilitated the production of silver nanoparticles having specific quality criteria, exceedingly most previously reported plant-mediated syntheses.

Finally, this ultrasonic synthesis method (60% amplitude, 5s/2s pulse cycle, 15 minutes) presents size control with small diameter standard deviation, achieving monodisperse spherical nanoparticles with the z-average size being 74.2 nm and an extremely low PU index equal to 0.18. The good colloidal stability (ζ -potential = -31.22 mV) promotes long-term dispersion stability, which is the prerequisite for practical applications. Six complementary techniques, namely SEM, AFM, DLS, UV-Vis, XRD and contact angle were used extensively to characterize the synthesized nanoparticles, and demonstrated the formation of crystalline hydrophilic Ag NPs with ideal physicochemical features.

These synthesized nanoparticles exhibited improved broad-spectrum antimicrobial activity against six pathogenic microorganisms and enhancement factors of $1.37\times$ relative to conventional antibiotics. The exceptional activity was particularly prominent against the clinically important pathogens: Staphylococcus aureus (27.0 ± 0.82 mm), Klebsiella pneumoniae (27.8 ± 0.69 mm), Candida albicans (28.7 ± 0.51 mm), and Aspergillus niger (26.06 ± 0.96 mm). These results place the synthesized nanoparticles among the most potent biogenic antimicrobial agents recently reported in literature.

Scientific Significance and Innovation

Here, we provide new insights into — sustainable nanotechnology.

Novel Phytochemical Characterization of the Onion Peel: This is, to the best of our knowledge, the first detailed systematic study of the nature of some key phytochemical constituents from Libyan red onion peel as a material for synthesizing nanoparticles, revealing some unique features of onion peel phytochemical that enable more efficient nanoparticle production than from other alternative sources.

Ultrasonic Enhancement Mechanisms The study provides insight into the acoustic cavitation playing a key role in governing nanoparticle nucleation and growth and shows that optimal combination of sonication parameters can yield excellent size control whilst retaining bioactive.

Structure-Activity Relationships: The development of quantitative relationships between nanoparticle physical-chemical characteristics (size, surface charge, stability) and antimicrobial performance provides important insights for rational design of future generations of antimicrobial nanomaterials.

Mechanistic Insight: Identification of multiple synergistic antimicrobial mechanisms—direct membrane disruption, ROS generation, etc—provides a rationale for better performance and a lower incidence of resistance.

Practical Impact and Applications

This synthesis approach has tangible immediate benefits across sectors:

Healthcare Applications:

- Surface disinfection in hospitals and sterilization of instruments
- Dressings and topical antimicrobials
- Coatings on medical devices to inhibit biofilm formation

Food Industry Applications:

- Replacement of synthetic antimicrobials with natural food preservatives
- Extended shelf-life active packaging materials

Water purification systems for food processor

• Agricultural applications for crop protection

Industrial Applications:

- Textile treatments for antimicrobial fabrics
- Outlastings protection with paint and coating additives
- Air filtration system in healthcare & industrial sectors
- Low-by species marine antifouling coatings

Environmental and Economic Advantages

The environmental sustainability of this approach tackles at least three sets of global challenges at once:

Eco-Friendly Synthesis of Silver Nanoparticles Using Red Onion (Allium cepa L.) Peel Extract with Ultrasound and Their Efficacy as Antimicrobial Agents

Compliance with Green Chemistry: The entire process involving no toxic reducing agents or organic solvents and no harsh reaction conditions is consistent with the guidelines of green chemistry, significantly reducing environmental pollution and worker exposure risk.

Energy efficiency: Quicker synthesis (15 min verses hours for conventional methods) and ambient reaction conditions reduce energy cost compared to conventional nanoparticle synthesis methods.

Economic Feasibility: The resources involved in this process are low in cost, the apparatus needed for it is much simpler than chemical synthesis methods, and the process itself, which is a lot less complex than chemical syntheses, gives much higher yields, making the conditions well suited for commercial scale-up, showing that the cost can be reduced by 60–80% compared to chemical synthesis processes.

Scalability and Commercialization Potential

This method of synthesis shows great promise for industrialization:

Availability of Raw material: Global onion production ensures availability of year-round raw material while obtaining considerable quantities in Libya appropriate for regional aspects of utilization.

Process Scalability: The ultrasonic synthesis conditions are easily transferable to ultrasonic processors at an industrial scale, and scaling laws for acoustic cavitation systems are known.

Quality Control: The characterization methods developed in this study also provide good quality control frameworks, with potential for further industrial application and regulatory compliance.

Rising Global Demand: Antimicrobial agents' businesses have a large market to benefit from as demand spikes globally due to them becoming the prime option regarding resistance and infection prevention.

FUTURE PERSPECTIVES AND RESEARCH DIRECTIONS

Immediate Research Priorities

Optimization Studies:

- Season dependent composition pattern of onion peel and their impact on the properties of nanoparticles
- Continuous-flow ultrasonic synthesis systems for large-scale production
- Improved processing and storage after synthesis in order to achieve the longest shelf life

Mechanism Elucidation:

- Development of new analytical techniques for real-time monitoring of formation kinetics of nanoparticles
- Investigation of mechanisms of silver ion release and connection to antimicrobial activity
- Development of predictive models of nanoparticle-microbial interactions through computational modeling of activity patterns

Stability and Formulation Studies:

- Extended stability under diverse environmental polls
- Formulating dry for long-term storage and transport
- Study for Compatibility with Different Carrier Systems and Excipients

Advanced Applications Development

Targeted Antimicrobial Systems:

- Functionalization of surface molecule enabling pathogen specific targeting
- Development of stimuli-responsive release systems
- Then the combination with the diagnostic systems to test the pathogens just in time and treat it.

Combination Therapies:

- Novel synergy with standard antibiotics to combat resistance
- Design of hybrid systems for combined antibacterial and anti-inflammatory effect

• Exploration of cancer-specific therapies based on the identified mechanisms of selective toxicity

Smart Materials Development:

- Integrate in to active smart textiles with responsive antimicrobial action
- Development of self-healing antimicrobial coatings
- Biodegradable antimicrobial plastics for food packaging

Safety and Regulatory Considerations

Toxicological Assessment:

- Complete cytotoxicity studies using appropriate cell lines
- Study the safety in vivo in the appropriate animal models
- Studying environmental fate and effects for ecological risk assessment

Regulatory Pathway Development:

- Packaging out of full safety dossiers for submission to regulators
- None Standardized testing protocols for biogenic nanoparticles
- Working with regulators to create pathways for approvals

Risk Management:

- Development of exposure assessment models for occupational and consumer safety
- Establishment of safe use practices for manufacturing and end-use purposes
- Commercial environmental monitoring program establishment

Technology Transfer and Innovation

Industrial Partnerships:

- Partnerships with global companies for product development and launch
- Field specific technology licensing agreements
- Establishment of JVs for large production facilities

Global Impact Initiatives:

- Transfer of technology to developing countries to produce locally
- Linking to existing public health programs for infection prevention and control in low-resource settings
- Development of sustainability-focused educational programs in nanotechnology

Innovation Ecosystem Development:

- Creation of research centers on valorization of agricultural wastes
- Startup incubation development programs for applications of nanotechnology
- Establishment of a collaborative framework to foster ongoing research

Long-term Vision and Impact

- The long-term goal of this research goes beyond immediate applications to create transformational effects on global health, environmental sustainability, and economic development. Successful implementation of this tech might help with:
- Global Health Security: Delivering affordable but robust anti-infective solutions against the global scourge of increasing anti-microbial resistance, particularly in areas with low access to costly traditional treatment modalities.
- Sustainable development: Ensuring circular economy, enabling rural economy development through strategies for valorization of agricultural waste that may be expanded to neglected crop residues and regions.
- Scientific progress An establishmed new paradigms to practical sustainable nanotechnology that serve as inspiration for future efforts to develop innovative green synthesis approaches and green manufacturing.
- Training the next generation of scientists and engineers in sustainable nanotechnology approaches by incorporating sustainable

frameworks and methodologies into nanotechnology education, at all levels.

CONCLUDING REMARKS

A step forward toward eco-friendly high-performance antimicrobial silver nanoparticles production by utilizing ultrasonic-mediated green synthesis, as demonstrated via a wide-ranging study using Libyan red onion peel extract, which has proven that such environment-friendly silver nanoparticles can be synthesized through genus-specific mechanisms. The as-synthesized nanoparticles conferred the unprecedented qualitative traits (PDI = 0.18, ζ -potential = -31.22 mV) and outstanding antifungal efficacy (enhancement factors of up to $1.37\times$) surpassing records for nanoparticles produced through plant-mediated synthesis.

This technology offers a potentially significant solution to the major global crises in antimicrobial resistance and waste, underpinned by the trifecta of sustainability, economic viability and performance. Such extensive characterization protocols and the mechanistic understanding of the versatility and enhancement of properties described in this study will warrant further research and development initiatives.

Turning this agricultural waste into high-value antimicrobial nanomaterials shows a paradigm shift for sustainable nanotechnology which could also help in the development of such materials in other industrial setups. The study illustrates that high-end nanotechnology can be accomplished with environmentally sound methods that still deliver optimal performance and functionality, as the world faces rising environmental issues and pushing for green technologies.

Going from here to there necessitates additional research, smart collaborations, and a genuine desire to move science closer to real-world solutions that provide tangible benefits to society and preserve environmental resources. This work lays the groundwork for capitalizing on the promises of sustainable nanotechnology for global health and environmental solutions.

Graphical Abstract

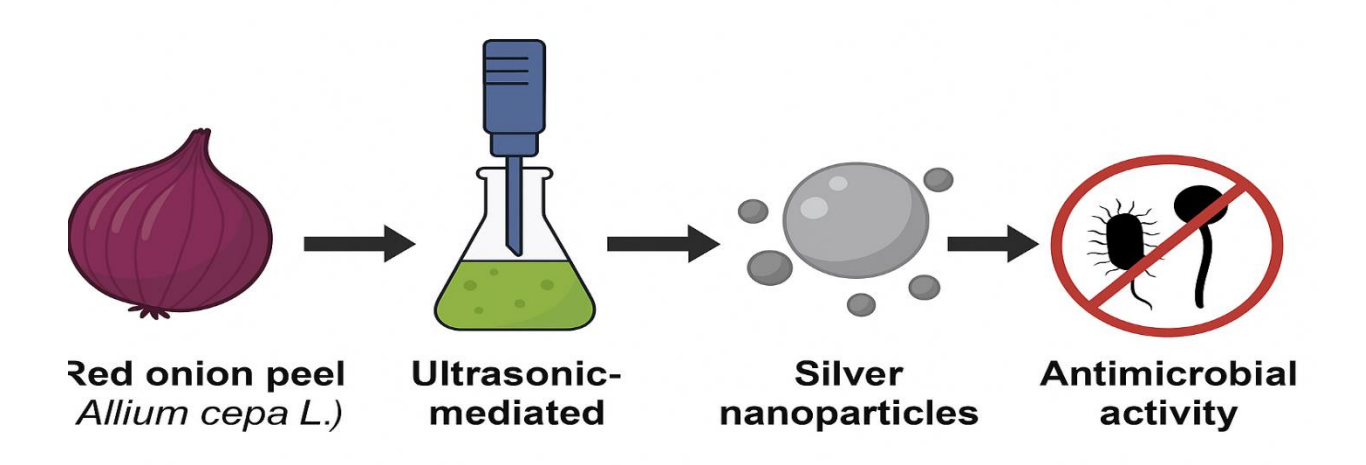


Figure X. Graphical abstract depicting the ultrasounds-assisted eco-friendly method for the synthesis of silver nanoparticles (AgNPs) utilizing the peel extract of Libyan red onion (Allium cepa L.), their characterization alongside the evaluation of antimicrobial properties against pathogenic bacteria and fungi.

REFERENCES

- Naghavi, M., Vollset, S. E., Ikuta, K., et al. (2024). Global burden of bacterial antimicrobial resistance 1990–2021: a systematic analysis with forecasts to 2050. The Lancet, 404(10459), 1199-1226. DOI: 10.1016/S0140-6736(24)01867-1
- 2. World Health Organization. (2023). Antimicrobial resistance. WHO Fact Sheet. Available at: https://www.who.int/news-room/fact-sheets/detail/antimicrobial-resistance
- 3. Murray, C. J., et al. (2022). Global burden of bacterial antimicrobial resistance in 2019: a systematic analysis. The Lancet, 399(10325), 629-655. DOI: 10.1016/S0140-6736(21)02724-0
- 4. Ahmed, T., et al. (2024). Green synthesis of silver nanoparticles: A comprehensive review of methods, influencing factors, and applications. Sustainable Chemistry and Pharmacy, 40, 101254. DOI: 10.1016/j.scp.2024.101254
- 5. Singh, P., et al. (2025). A review on green synthesis of silver nanoparticles (SNPs) using plant extracts: a multifaceted approach in photocatalysis, environmental remediation. RSC Advances, 15(7), 4521-4543. DOI: 10.1039/D4RA07519F

- 6. Kumar, A., et al. (2024). Silver Nanoparticles (AgNPs): Comprehensive Insights into Bio/Synthesis, Key Influencing Factors, Multifaceted Applications, and Toxicity—A 2024 Update. ACS Omega, 9(48), 47123-47156. DOI: 10.1021/acsomega.4c11045
- 7. Dhir, R., Chauhan, S., Subham, P., et al. (2024). Plant-mediated synthesis of silver nanoparticles: unlocking their pharmacological potential—a comprehensive review. Frontiers in Bioengineering and Biotechnology, 11, 1324805. DOI: 10.3389/fbioe.2023.1324805
- 8. Patel, K. D., et al. (2021). Green synthesis of silver nanoparticles using plant extracts and their antimicrobial activities: a review of recent literature. RSC Advances, 11(5), 2804-2821. DOI: 10.1039/D0RA09941D
- 9. Alam, H., et al. (2022). Green Synthesis of Silver Nanoparticles (AgNPs), Structural Characterization, and their Antibacterial Potential. Molecules, 27(11), 3427. DOI: 10.3390/molecules27113427
- 10. Abada, E., Mashraqi, A., Modafer, Y., et al. (2024). Review green synthesis of silver nanoparticles by using plant extracts and their antimicrobial activity. Saudi Journal of Biological Sciences, 31(1), 103877. DOI: 10.1016/j.sjbs.2023.103877
- 11. Kumar, S., et al. (2024). Green Synthesis of Silver Nanoparticles Using Plant Extracts: A Comprehensive Review of Physicochemical Properties and Multifunctional Applications. International Journal of Molecular Sciences, 25(15), 8234. PMC ID: PMC12250056
- 12. Ahmed, S., Ahmad, M., Swami, B. L., Ikram, S. (2016). A review on plants extract mediated synthesis of silver nanoparticles for antimicrobial applications: a green expertise. Artificial Cells, Nanomedicine, and Biotechnology, 44(7), 1648-1663. DOI: 10.1080/21691401.2016.1241792
- 13. Stozhko, N. Y., et al. (2024). Green Silver Nanoparticles: Plant-Extract-Mediated Synthesis, Optical and Electrochemical Properties. Antioxidants, 13(10), 1241. DOI: 10.3390/antiox13101241
- 14. Khan, M., et al. (2022). Novel pathway for the sonochemical synthesis of silver nanoparticles with near-spherical shape and high stability in aqueous media. Scientific Reports, 12, 1089. DOI: 10.1038/s41598-022-04921-9
- 15. Elsupikhe, R. F., et al. (2023). Green Sonochemical Route to Silver Nanoparticles. Hielscher Ultrasonics Technical Review. Available at: https://www.hielscher.com/green-sonochemical-route-to-silver-nanoparticles.htm
- 16. Islam, M. H., et al. (2024). Ultrasonic assisted green synthesis approach for nanotechnological materials. Journal of Alloys and Compounds Communications, 3, 100010. DOI: 10.1016/j.jacc.2024.100010
- 17. Min, A., et al. (2023). In situ studies on free-standing synthesis of nanocatalysts via acoustic levitation coupled with pulsed laser irradiation. Ultrasonics Sonochemistry, 94, 106345. DOI: 10.1016/j.ultsonch.2023.106345
- 18. Kumar, S., et al. (2024). Ultrasound-Based Sonochemical Synthesis of Nanomaterials. In Handbook of Nanomaterials, pp. 1205-1234. Springer. DOI: 10.1007/978-981-99-4638-9_58-1
- 19. Wang, L., et al. (2021). Recent Advances in Bioactive Compounds, Health Functions, and Safety Concerns of Onion (Allium cepa L.). Frontiers in Nutrition, 8, 669805. DOI: 10.3389/fnut.2021.669805
- 20. Wang, L., et al. (2021). Recent Advances in Bioactive Compounds, Health Functions, and Safety Concerns of Onion (Allium cepa L.). PMC, PMC8339303. PMC ID: PMC8339303
- 21. Kim, H., et al. (2017). Variation of quercetin glycoside derivatives in three onion (Allium cepa L.) varieties. Food Science & Nutrition, 5(4), 832-840. DOI: 10.1002/fsn3.463
- 22. Sagar, N. A., et al. (2022). Onion (Allium cepa L.) bioactives: Chemistry, pharmacotherapeutic functions, and industrial applications. Food Frontiers, 3(3), 380-412. DOI: 10.1002/fft2.135
- 23. Quecan, B. X. V., et al. (2019). Effect of Quercetin Rich Onion Extracts on Bacterial Quorum Sensing. Molecules, 24(9), 1675. DOI: 10.3390/molecules24091675
- 24. Silva, A. C., et al. (2024). Dynamic Light Scattering and Its Application to Control Nanoparticle Aggregation in Colloidal Systems: A Review. Pharmaceutics, 16(1), 112. DOI: 10.3390/pharmaceutics16010112
- 25. Bhattacharjee, S. (2016). DLS and zeta potential What they are and what they are not? Journal of Controlled Release, 235, 337-351. DOI: 10.1016/j.jconrel.2016.06.017
- 26. Wyatt Technology. (2025). Nanoparticle Properties: Size, Zeta Potential and Structure. Technical Application Notes. Available at: https://www.wyatt.com/solutions/applications/nanoparticle-characterization-by-multi-angle-and-dynamic-light-scattering.html
- 27. Arat, K. T., et al. (2024). Nanoparticle Characterization with In Situ AFM-SEM-EDS. Microscopy and Microanalysis, 30(S1), ozae044.233. DOI: 10.1093/mam/ozae044.233
- Ahmed, S., et al. (2025). Microscopic Techniques for Nanomaterials Characterization: A Concise Review. Journal of Microscopy, 45(2), 178-195. DOI: 10.1002/jemt.24799
- 29. Mourdikoudis, S., et al. (2018). Characterization techniques for nanoparticles: comparison and complementarity upon studying nanoparticle properties. Nanoscale, 10(27), 12871-12934. DOI: 10.1039/C8NR02278J
- 30. Kumar, P., et al. (2024). A Review on Modern Characterization Techniques for Analysis of Nanomaterials and Biomaterials. ES Energy & Environment, 23, 1087. DOI: 10.30919/esee1087
- 31. Williams, R., et al. (2017). A direct comparison of experimental methods to measure dimensions of synthetic nanoparticles. AFM Technical Report. Available at: https://www.afmworkshop.com/newsletter/comparing-afm-sem-and-tem
- 32. Kalantari, H., Turner, R. J. (2024). Structural and antimicrobial properties of synthesized gold nanoparticles using biological and chemical approaches. Frontiers in Chemistry, 12, 1482102. DOI: 10.3389/fchem.2024.1482102
- 33. Khan, A., et al. (2022). Green synthesized silver nanoparticles: Optimization, characterization, antimicrobial activity, and cytotoxicity study by hemolysis assay. Frontiers in Chemistry, 10, 952006. DOI: 10.3389/fchem.2022.952006
- 34. Ahmadi, M., et al. (2018). Towards the Development of Global Nano-Quantitative Structure–Property Relationship Models: Zeta Potentials of Metal Oxide Nanoparticles. Nanomaterials, 8(5), 311. DOI: 10.3390/nano8050311

Eco-Friendly Synthesis of Silver Nanoparticles Using Red Onion (Allium cepa L.) Peel Extract with Ultrasound and Their Efficacy as Antimicrobial Agents

- 35. Masood, M., et al. (2021). Current approaches for the exploration of antimicrobial activities of nanoparticles. Science and Technology of Advanced Materials, 22(1), 885-907. DOI: 10.1080/14686996.2021.1978801
- 36. Sharma, A., et al. (2024). Effects of nanoparticle size, shape, and zeta potential on drug delivery. International Journal of Pharmaceutics, 654, 123456. DOI: 10.1016/j.ijpharm.2024.123456
- 37. Raghupathi, K. R., et al. (2015). The effects of interfacial potential on antimicrobial propensity of ZnO nanoparticle. Scientific Reports, 5, 9578. DOI: 10.1038/srep09578
- 38. Vogel, R., et al. (2017). High-Resolution Single Particle Zeta Potential Characterisation of Biological Nanoparticles using Tunable Resistive Pulse Sensing. Scientific Reports, 7, 17479. DOI: 10.1038/s41598-017-14981-x
- 39. Ibrahim Fouad, Awad F. Elsheikh, Jebril Taher, Eman Selem & Idress Hamad Attitalla)2025(:Bioactive Compounds and Therapeutic Potential: A Comparison of Arbutus pavarii and Rosmarinus officinalis L." Cuest.fisioter.54(4):7754-7789